AAS 14-414

SAFE RELEASE OF A PICOSATELLITE FROM A SMALL SATELLITE CARRIER IN LOW EARTH ORBIT

Martin Wermuth[*], Gabriella Gaias[†], and Simone D'Amico[‡]

The BIROS satellite, which is scheduled for launch in 2015 into a low Earth orbit, will carry onboard a picosatellite and subsequently release it through a spring mechanism with a fixed velocity. In the frame of the AVANTI experiment, the BIROS satellite will perform proximity maneuvers in a mid-range formation with the picosatellite, based solely on optical navigation through its onboard camera. Therefore it is necessary to keep the relative distance of the two spacecraft within certain limits. This is contradicted by the fact, that the spring mechanism is designed to create a large and safe separation between the two spacecraft.

In this paper a maneuver strategy is developed in the framework of relative orbital elements. The goal is to avoid any risk of collision on one side and to mitigate the possibility of formation evaporation on the other side. Main design drivers are several uncertainties - most prominently the performance uncertainty of the release mechanism. The analyzed strategy consists of two maneuvers: the separation itself and a drift reduction maneuver of the BIROS satellite after 1.5 revolutions. Afterwards a third maneuver is to be performed to minimize the residual drift, estimated through an orbit determination with radar tracking.

The selected maneuver parameters are validated in a Monte Carlo simulation. It is demonstrated that the risk of formation evaporation is below 0.1% as well as the eventuality of a residual drift towards the carrier. In the latter case formation safety is guaranteed by a passive safety achieved through a proper relative eccentricity/inclination vector separation.

INTRODUCTION

This paper addresses the design of a safe strategy to inject a picosatellite in low Earth orbit after separation from a small satellite carrier. The problem is motivated by the Autonomous Vision Approach Navigation and Target Identification (AVANTI) experiment onboard the Berlin InfraRed Optical System (BIROS[1]) spacecraft.

In the recent years, the deployment of small-scale satellites as secondary payloads into low Earth orbit has become more and more common.[2,3,4,5] To this trend contributed both the miniaturization of the technology and the increase in number of educational scientific programs. Within these applications, the launcher vehicles are typically equipped by spring-based deployment devices which provide a linear velocity relative to the carrier that ranges from 0.3 to 2.0 m/s.[6] Since the main purpose of these technology demonstrations is focused on the ejected elements, the separation phase

[*]Research Engineer, German Space Operations Center (GSOC/DLR), Oberpfaffenhofen , 82234 Wessling, Germany.
[†]Research Engineer, German Space Operations Center (GSOC/DLR), Oberpfaffenhofen , 82234 Wessling, Germany.
[‡]Assistant Professor, Department of Aeronautics & Astronautics, Stanford University, Durand Building, Stanford, CA 94305, USA.

has to quickly and safely establish a certain relative distance, disregarding how different the final dynamics of the two vehicles are. Therefore, the ejection can be simply achieved by imparting the deployment delta-v in flight direction, in the verse dictated by the differential drag effect.

In 2010, in the frame of the Prototype Research Instruments and Space Mission technology Advancement (PRISMA[7]) mission, a different application scenario was successfully demonstrated in flight. It involved the separation of two satellites with the aim of performing some formation flying activities. The employed separation mechanism, a 3-point system with hooks and clamps kept in locked position by a single wire, was meant to provide a small delta-v (i.e., nominally 0.12 m/s).[8] Moreover, the accuracy of its true performance allowed considering safe relative orbits that intersect the local carrier horizon plane at an along-track separation of the order of 150 m. A further peculiarity of this satellite separation resided in the availability of a GPS-receiver on each satellite and of an inter-satellite link. Thus, the differential GPS relative navigation could be used to estimate both the deployment delta-v and the residual drift at the end of the separation phase.

The problem we are dealing with, presents commonalities with both these above mentioned categories of applications. On one hand, the BIROS spacecraft makes use of a spring-based Picosatellite Orbit Deployer (POD) device that provides a large and strongly uncertain separation delta-v. On the other hand, the picosatellite release serves the sake of the AVANTI experiment, where a noncooperative target (i.e., the ejected picosatellite) is the object of several formation flying activities.
The major challenges of our application stem from the fact that a safe and stable relative motion of the formation has to be established shortly after separation subject to several operational constraints. Nevertheless, the results of this paper allow the extension and generalization of the relative eccentricity/inclination vector separation method[9] to a new class of distributed space systems. Overall this work proposes an effective way to solve a mission specific problem which might have relevant applications in future on-orbit servicing and distributed space systems architectures.

The proposed and analyzed guidance and maneuver planning approach is based on the relative eccentricity/inclination vector separation method which was first introduced for the collocation of geostationary satellites,[10] later applied for long-range rendezvous in low Earth orbits,[11] and finally extended to formation-flying[12] and on-orbit servicing scenarios.[13] Indeed a safe passively stable relative motion can be established after the release of a picosatellite from a satellite carrier by ensuring the (anti-) parallelism of the relative eccentricity and inclination vectors.
A further novelty of the proposed approach is to investigate, at a design level, how additional relevant operational aspects impact the safety and the feasibility of the guidance plan. Specifically, our study addresses also the distance of the nearest transit of the picosatellite through the local along-track axis, the eventual delay and/or mis-execution of the drift-stopping maneuver, and, finally, the achievement of a final relative drift with known and safe direction, regardless of the uncertainties in the whole control chain.
In order to deal with such a comprehensive scenario while establishing a desired passively safe stable relative orbit, the preliminary design of the maneuvering strategy is carried out in the Relative Orbital Elements (ROE) framework.[14] These parameters, in fact, are the integration constants of the Hill-Clohessy-Wiltshire equations and provide a direct insight into the geometry and thus into the safety characteristics of the relative motion. By making use of the simple relations between changes in ROE and applied delta-v derived from the inversion of the model of relative dynamics, a nominal scheme of maneuvers to accomplish the separation can be designed. Specifically it can be shown that a single maneuver cannot establish the parallelism of the relative eccentricity and inclination vectors, within the operational constraints of the application under consideration. A

double-maneuver strategy, on the contrary, can accomplish this task, leaving as degrees of freedom the tuning of certain parameters related to the size and mean along-track separation of the final relative orbit and to the satisfaction of the aforementioned feasibility aspects.

The ultimate validation of the preliminary designed guidance scheme is accomplished through multiple numerical analyses. These take into account several sources of uncertainty which affect the reliability of the nominal plan: the POD delta-v magnitude error due to the spring release mechanism, the BIROS attitude control error, the BIROS maneuver execution error, and the uncertainty in the knowledge of the differential ballistic coefficients. Taking all these uncertainties into account it is obvious, that after the second maneuver a residual drift will remain, though in the safe direction prescribed by the preliminary design. Therefore, in order to achieve a stable formation for the start of the AVANTI experiment, an orbit determination of the picosatellite has to be performed and a third maneuver has to be executed to stop the residual drift.

In the following, first an overview of the mission with its requirements is provided. Secondly, the preliminary design of the guidance plan is described and a baseline scenario compliant with all the relevant operational aspects is selected. Finally, the results of some nonlinear Monte Carlo (MC) simulations are presented and discussed, in the attempt to demonstrate the safety and efficiency of the overall methodology.

MISSION OVERVIEW AND REQUIREMENTS

Scheduled for launch in 2015 the BIROS satellite (60x80x80 cm, 140 kg) will be operated by the German Aerospace Center (DLR). Its primary task next to several technology demonstration experiments (including AVANTI) will be the observation of wildfires in the frame of the FireBird mission. Together with the similar TET-1 satellite, which was launched in 2012 and is operated by DLR as well, it will form a loose constellation of Earth observation satellites. BIROS is designated for injection into a sun-synchronous orbit with 9:30 LTAN at an orbit height of 515 km. The spacecraft is equipped with a propulsion system and a fuel availability corresponding to circa 20 m/s of delta-v. Half of the fuel is allocated to the AVANTI Experiment, while the other half is allocated for the primary mission objective.

The AVANTI experiment is intended to demonstrate vision-based noncooperative autonomous approaches and recedes operations of an active small satellite (BIROS) within separations between 10 km and 100 m from a picosatellite (10x10x10 cm, 1kg) making use of angles-only measurements. The picosatellite is originally carried by BIROS and later on ejected through a POD deployer after the successful check-out and commissioning of all relevant BIROS subsystems. The AVANTI experiment is intended to start after that the BIROS/Picosatellite formation has been brought to an initial safe configuration at about 5 km separation with minimal residual drift in along-track direction. This delicate operational task is solely ground-based and performed by the Flight Dynamics Services (FDS) division of the German Space Operations Center (GSOC), which is in charge of the orbit determination and control of the FireBird mission.

The mission profile is characterized by several external constraints which have to be considered during the analysis of a safe separation. First of all the separation must take place during a ground-station contact, which poses restrictions on the location of the deployment along the orbit and on the separation attitude for proper communication. The size of the delta-v imparted at injection is fixed to 1.41 m/s. If oriented in along-track direction, this corresponds to about 2.8 km semi-major axis difference between the BIROS and picosatellite orbits, which produces an along-track drift of

27 km/orbit or 405 km/day. Since the only means of navigation information for the picosatellite is radar tracking from ground, with associated latencies of typically 24 hours, the risk of formation evaporation would be too high when adopting this conventional separation strategy. Nevertheless, due to all the uncertainties that characterize the whole separation and control chain, a certain residual drift towards evaporation remains also when employing the guidance scheme proposed here. The radar tracking facility foreseen within the FireBird mission is the imaging radar (TIRA) station in Germany.[15] According to it, due to the different sizes of the BIROS satellite and the picosatellite, a minimum distance of 5 km is required for TIRA to be able to distinguish the signal from the two spacecraft. Typically two tracking passes with a spacing of 12 hours are necessary for an accurate orbit determination.

Additional geometrical constraints are introduced by the camera employed by the AVANTI experiment. The experience from previous missions[16] suggests, that the camera should be able to detect the picosatellite up to a distance of 10 km. The half field of view of the camera is 6.8° horizontally and 9.15° vertically. The separation scenario must ensure the visibility of the picosatellite at the start of the AVANTI experiment.

RELATIVE MOTION DESCRIPTION

The relative motion is parameterized by this set of dimensionless relative orbital elements (ROE):

$$\delta\boldsymbol{\alpha} = \begin{pmatrix} \delta a \\ \delta\lambda \\ \delta e_x \\ \delta e_y \\ \delta i_x \\ \delta i_y \end{pmatrix} = \begin{pmatrix} \delta a \\ \delta\lambda \\ \delta e\cos\varphi \\ \delta e\sin\varphi \\ \delta i\cos\theta \\ \delta i\sin\theta \end{pmatrix} = \begin{pmatrix} (a-a_\mathrm{d})/a_\mathrm{d} \\ u-u_\mathrm{d}+(\Omega-\Omega_\mathrm{d})\cos i_\mathrm{d} \\ e\cos\omega - e_\mathrm{d}\cos\omega_\mathrm{d} \\ e\sin\omega - e_\mathrm{d}\sin\omega_\mathrm{d} \\ i-i_\mathrm{d} \\ (\Omega-\Omega_\mathrm{d})\sin i_\mathrm{d} \end{pmatrix} \tag{1}$$

where a, e, i, Ω, and M denote the classical Keplerian elements and $u = M + \omega$ is the mean argument of latitude.* The subscript "d" labels the deputy spacecraft of the formation, which plays the role of the maneuverable carrier satellite (BIROS) and defines the origin of the local radial-tangential-normal (RTN) frame. Hereinafter, the magnitudes of the dimensionless relative eccentricity and inclination vectors are shortly quoted as $\|\delta\mathbf{e}\| = \delta e$ and $\|\delta\mathbf{i}\| = \delta i$ respectively, whereas the subscript is dropped, meaning that all the absolute orbital quantities appearing in the equations belong to the servicer satellite.
Under the assumptions of the Hill-Clohessy-Wilshire equations (HCW),[17] the quantities $a\delta e$ and $a\delta i$ provide the amplitudes of the in-plane and out-of-plane relative motion oscillations, whereas relative semi-major axis, $a\delta a$, and relative mean longitude, $a\delta\lambda = a(\delta u + \delta i_y \cot i)$, provide mean offsets in radial and along-track directions respectively.[9,18]

According to the model of the relative dynamics just introduced, the instantaneous dimensional variations of the ROE caused by an impulsive maneuver (or an instantaneous velocity change) at

*A section on mathematical notation is provided in the appendix.

the mean argument of latitude u_{M} are given by:

$$\begin{array}{lcccc} a\Delta\delta a & = & & +2\delta v_{\mathrm{T}}/n & \\ a\Delta\delta\lambda & = & -2\delta v_{\mathrm{R}}/n & & \\ a\Delta\delta e_x & = & +\delta v_{\mathrm{R}}\sin u_{\mathrm{M}}/n & +2\delta v_{\mathrm{T}}\cos u_{\mathrm{M}}/n & \\ a\Delta\delta e_y & = & -\delta v_{\mathrm{R}}\cos u_{\mathrm{M}}/n & +2\delta v_{\mathrm{T}}\sin u_{\mathrm{M}}/n & \\ a\Delta\delta i_x & = & & & +\delta v_{\mathrm{N}}\cos u_{\mathrm{M}}/n \\ a\Delta\delta i_y & = & & & +\delta v_{\mathrm{N}}\sin u_{\mathrm{M}}/n \end{array} \tag{2}$$

where n indicates the mean motion of the servicer and the delta-v is expressed in the RTN frame:

$$\delta\mathbf{v} = (\delta v_{\mathrm{R}}, \delta v_{\mathrm{T}}, \delta v_{\mathrm{N}})^{\mathrm{T}} \tag{3}$$

Before the release of the picosatellite, the relative state $a\delta\boldsymbol{\alpha}$ is null. Then, if a single separation maneuver is executed at the mean argument of latitude u_1, the following ROE variations can be established at $u = u_1$:

$$\begin{cases} na\Delta\delta a &= 2\delta v_{\mathrm{T}} \\ na\Delta\delta\lambda &= -2\delta v_{\mathrm{R}} \\ na\Delta\delta e &= \sqrt{\delta v_{\mathrm{R}}^2 + 4\delta v_{\mathrm{T}}^2} \\ \tan(u_1 - \xi) &= \dfrac{\delta v_{\mathrm{R}}}{2\delta v_{\mathrm{T}}} \\ na\Delta\delta i &= |\delta v_{\mathrm{N}}| \\ \tan(u_1) &= \dfrac{\Delta\delta i_y}{\Delta\delta i_x} \end{cases} \tag{4}$$

where ξ denotes the obtained phase angle of the relative eccentricity vector.
As mentioned above, both location and magnitude of the first separation maneuver are fixed by the need of performing it during a given ground contact making use of a POD device. This poses the following constraint on the magnitude of the separation maneuver:

$$\delta v = \|\delta\mathbf{v}\| = \sqrt{\delta v_{\mathrm{R}}^2 + \delta v_{\mathrm{T}}^2 + \delta v_{\mathrm{N}}^2} \tag{5}$$

and the number of effective degrees of freedom of the problem is reduced so that one can satisfy only two of the conditions of Eq. (4).
By analyzing the obtainable relative motion within the requirements of our application scenario, it can be proven that:

- if $\delta v_{\mathrm{T}} = 0$, the established relative motion is characterized by $\delta\mathbf{e}^{\mathrm{T}}\delta\mathbf{i} = 0$ [see Eq. (2)]. In other words, radial and cross-track maneuvers at the same location produce perpendicular relative eccentricity and inclination vectors. Thus the minimum separation in the R–N plane is null, which is not acceptable for safety reasons.[12]
- if $\delta v_{\mathrm{T}} \neq 0$, the phase of $\delta\mathbf{e}$ can be changed but not as much as achieving an exact (anti) parallelism of the relative eccentricity/inclination vectors after only one maneuver is executed.

It is emphasized that, in order to avoid a collision, it is necessary to establish a certain drift in the relative motion through the first separation maneuver (i.e., δv_{T} must be $\neq 0$). In this case, in fact, the first passage of the deputy satellite across the along-track axis will occur after some separation is built up.
In conclusion, since it is not possible to achieve passive safety by accomplishing a single separation maneuver, at least a second maneuver must be performed, as addressed in the following section.

Separation preliminary design: the double-maneuver scheme

The analytical form of the general expression of the in-plane double-pulse maneuvers' scheme, for whatever aimed final conditions, as function of the mean arguments of latitude of the two maneuvers is given in Eq.(15) of Reference 14. Nevertheless, this expression is quite complicated and does not allow an immediate geometrical insight into the geometry of the relative motion. To this aim, at a preliminary stage, we can use Eq.(2.42) of Reference 9:

$$\begin{array}{rcccccccccc}
\delta v_{\mathrm{R1}} &=& \frac{na}{2}\,(& -\frac{\Delta\delta\lambda^*}{2} & +\Delta\delta e\,\sin(u_1-\xi) &) - \frac{na}{2}\kappa\,(& \Delta\delta a & -\Delta\delta e\,\cos(u_1-\xi) &) \\
\delta v_{\mathrm{T1}} &=& \frac{na}{4}\,(& +\Delta\delta a & +\Delta\delta e\,\cos(u_1-\xi) &) - \frac{na}{4}\kappa\,(& \frac{\Delta\delta\lambda^*}{2} & +\Delta\delta e\,\sin(u_1-\xi) &) \\
\delta v_{\mathrm{R2}} &=& \frac{na}{2}\,(& -\frac{\Delta\delta\lambda^*}{2} & -\Delta\delta e\,\sin(u_1-\xi) &) + \frac{na}{2}\kappa\,(& \Delta\delta a & -\Delta\delta e\,\cos(u_1-\xi) &) \\
\delta v_{\mathrm{T2}} &=& \frac{na}{4}\,(& +\Delta\delta a & -\Delta\delta e\,\cos(u_1-\xi) &) + \frac{na}{2}\kappa\,(& \frac{\Delta\delta\lambda^*}{2} & +\Delta\delta e\,\sin(u_1-\xi) &)
\end{array} \tag{6}$$

with

$$\kappa = \frac{\sin\Delta u}{\cos\Delta u - 1} \qquad \Delta u = u_2 - u_1 \qquad \xi = \arctan\left(\frac{\Delta\delta e_y}{\Delta\delta e_x}\right) \tag{7}$$

As mentioned in the previous section, since the initial relative state is null, the total aimed variation coincides with the final aimed relative state:

$$\Delta\delta\bullet = \delta\,\bullet_{\mathrm{F}} \qquad \text{and} \qquad \varphi_{\mathrm{F}} = \xi \tag{8}$$

Equation (6) provides an analytical expression of the double-impulse in-plane scheme to achieve a prescribed total variation of $\Delta\delta a$, $\Delta\delta\mathbf{e}$, and $\Delta\delta\lambda^*$. It embodies a simplification of the ones in Reference 14, since it does not involve the relationship between $\delta\lambda$ and δa, leading to the quantity $\Delta\delta\lambda^*$ instead of the truly obtainable $\Delta\delta\lambda$. However this is acceptable at a preliminary stage, and allows achieving a much simpler expression of the in-plane delta-vs.

When dealing with the in-orbit release of a satellite, Eq. (6) must be complemented with the out-of-plane equations. The passive safety constraint of final (anti)parallelism of the relative e/i vectors, in fact, couples back to the impulsive reconfiguration problem.
In the following, the remaining specific requirements of the separation problem are listed and discussed, together with their geometrical interpretation in the ROE space. In Figure 1 all the final desired quantities, which are the parameters that appear in Eq. (6) are marked in black. The other quantities represent the intermediate values obtained during the execution of a double-impulse maneuvering scheme.

The following features characterize our application scenario:

- The location of the first maneuver u_1 is fixed and known, since the deployment has to occur during a ground contact. Consequently, the phase of the relative inclination vector after the first maneuver θ is also fixed (i.e., dotted light gray segment in the $\delta\mathbf{i}$ plane): $u = u_1 = \theta_{\mathrm{F}}$.

- In order to achieve passive safety, we must impose the phase of the final $\delta\mathbf{e}$, ξ to be equal to θ_{F} (i.e., dotted light gray segment in the first quadrant of $\delta\mathbf{e}$ plane), or to $\theta_{\mathrm{F}} + \pi$ (i.e., third quadrant). Thus, in a general case, we can impose $\xi = \theta_{\mathrm{F}} + \eta$, where the service parameter η can only assume the values of 0 or π

- Our aim is to establish a final stable relative orbit, thus $\delta a_{\mathrm{F}} = 0$. This implies that all terms in $\Delta\delta a$ in Eq. (6) vanish.

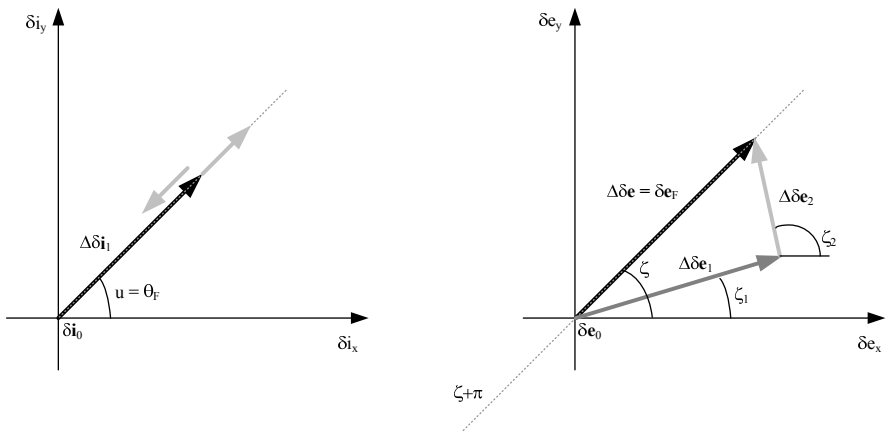

Figure 1. Sketch in the ROE space of the maneuvering scheme of Eq. (6) **to achieve passive safety**

- Equation (6) is defined for $\Delta u \neq 0$ or $\neq 2\pi$. In all other cases, κ weights the effect of the maneuvers' spacing on the final four in-plane delta-v expressions. In the special case of κ odd number and $\Delta u = \kappa\pi$ the second part of Eq. (6) vanishes. As a result the delta-v expressions are characterized by a symmetrical form. Moreover, in these particular locations of the second maneuver, the effect of the second out-of-plane maneuver can only change the magnitude of δi, and not the phase θ_{F}, whenever δv_{N2} is nonzero. This is marked by the gray arrows in the left side of Figure 1.

- As already mentioned, the first maneuver is accomplished by the deployment device, thus its magnitude is constrained to δv. This introduces a relationship on the three RTN components, and, consequently on the achievable $\Delta\delta e$, $\Delta\delta\lambda^*$, and $\Delta\delta i$.

By taking into account the aforementioned requirements, the delta-v expressions of Eq. (6) simplify to:

$$\begin{array}{rcl} \delta v_{\mathrm{R1}} & = & -\frac{na}{4}\left(\quad \Delta\delta\lambda^* \quad\right) \\ \delta v_{\mathrm{T1}} & = & \pm\frac{na}{4}\left(\quad \Delta\delta e \quad\right) \\ \delta v_{\mathrm{R2}} & = & -\frac{na}{4}\left(\quad \Delta\delta\lambda^* \quad\right) \\ \delta v_{\mathrm{T2}} & = & \mp\frac{na}{4}\left(\quad \Delta\delta e \quad\right) \end{array} \tag{9}$$

since $u_1 = \xi$. The signs of Eq. (9) are determined by fixing η (i.e., the final $\delta\mathbf{e}/\delta\mathbf{i}$ configuration) and by the sign of $\Delta\delta\lambda^*$ (i.e., picosatellite leading or following the carrier).

Referring to Eq. (9), the remaining degrees of freedom of the separation problem are: two among the three aimed magnitudes δe_{F}, δi_{F} and $\delta\lambda^*_{\mathrm{F}}$ together with the spacing between the maneuvers (i.e., the number of half revolutions κ). These parameters are fixed as soon as an aimed final orbit is identified. Therefore, the next section deals with the identification of such a nominal baseline, in order to cope with some operative aspects of crucial importance in our realistic scenarios.

Baseline identification in compliance with the operative constraints

This section discusses how some operative constraints impact the degrees of freedom of the preliminary design formulation. Outcome is the identification of feasible baselines for the aimed rel-

ative orbit. An analysis and verification of their robustness with respect to system uncertainties is accomplished afterwards.

Table 1. Meaningful operative constraints for the in-orbit satellite release

Constraint	Identifier	Rational	Consequence
safety	1	TIRA tracking capability	$\lvert a\delta\lambda_{\mathrm{F}}\rvert \geq 5000$ m
safety	2	1st cross of the along-track axis	Given $\delta\lambda_{\mathrm{F}}$ fixes η
safety	3	Effect of differential drag	Choice of the direction of $\delta\lambda_{\mathrm{F}}$
safety	4	Delay of 2nd maneuver	No collision before passive safety achievement
safety	5	Passive safety	Given η, minimum size of δe_{F} and δi_{F}
safety	6	Sign of δa after 1st maneuver	$\lvert\delta v_{\mathrm{T1}}\rvert$ greater than spring error
safety	7	Truly obtainable $a\delta i$	aimed $\delta i > (\delta i_{\min} + \text{margin})$
visibility	1	Picosat camera detectability	$\lvert a\delta\lambda_{\mathrm{F}}\rvert \leq 10000$ m
visibility	2	Camera FOV in R direction	$a\delta e_{\max} < 596$ m at $a\delta\lambda_{\mathrm{F}} = 5000$ m
visibility	3	Camera FOV in N direction	$a\delta i_{\max} < 805$ m at $a\delta\lambda_{\mathrm{F}} = 5000$ m

Table 1 lists the main operative constraints that are involved in the in-orbit release of a satellite, as explained above.
Constraints safety #1 and visibility #1 determine the domain of the aimed relative mean longitude, that is the mean satellite separation in tangential direction.

Safety constraint #2 determines the parallel or anti-parallel $\delta\mathbf{e}/\delta\mathbf{i}$ configuration (i.e., η). In particular, if the picosatellite is released so that at the end of the separation it leads the carrier in flight direction, an instantaneous negative radial delta-v must be imparted (i.e., $\delta v_{\mathrm{R1}} < 0$). Therefore, in order to avoid an immediate crossing of the local along-track axis, the semi-major axis of the picosatellite shall be reduced (i.e., $\delta v_{\mathrm{T1}} < 0$) to drift towards positive along-track separations. This combination of signs in Eq. (9) is obtained with $\eta = \pi$ in Eq. (6), since $\xi = \theta_{\mathrm{F}} + \eta$. Thus the final aimed relative orbit must have anti-parallel relative e/i vectors.
The safe complementary situation (i.e., picosatellite released to follow the carrier) requires $\delta v_{\mathrm{R1}} > 0$ and a positive drift (i.e., $\delta v_{\mathrm{T1}} > 0$). According to our maneuvering scheme, this is obtained if $\eta = 0$, thus by establishing a parallel configuration.

The choice of having picosatellite leading/following BIROS can be taken by considering the safety constraints #3 and #4. They address the natural effect of the differential drag. In our application, the ballistic coefficient of the picosatellite is greater than that of BIROS, thus its orbit lowers faster, producing a drift at a relative level. Specifically, if the picosatellite is leading the carrier in flight direction, the natural drift tends towards larger separations. On the opposite situation, the picosatellite will tend to come back towards the carrier. The trade-off between *evaporation* or *proximity* shall take into account the constraint safety #4 as well. According to it, any dangerous situation before the accomplishment of the second maneuver shall be avoided. This is motivated by the fact that a single maneuver is not able to establish passive safety (see previous sections).

Therefore, in order to satisfy the first four safety requirements, according to our scenario, a final configuration with the picosatellite leading the carrier in positive tangential direction is to be preferred. Consequently, $\Delta\lambda_{\mathrm{F}} > 0$ and $\eta = \pi$. The range of feasible sizes of the aimed relative orbit are derived from the remaining constraints of Table 1.
Constraint safety #6 requires that the direction of the drift is unequivocally defined, disregarding the size of execution error of the first maneuver. Thus, by considering an error $\tilde{e}$ of magnitude 0.141 m/s (i.e., 10% of the total magnitude δv), the delta-v in tangential direction must produce a negative

Table 2. Admissible sizes of the final relative orbit

Aimed ROE	Min magnitude [m]	Max magnitude [m]
$\delta\lambda$	5000	10000
δe	512	596
δi	278	805

drift in any case. This implies:

$$|\delta v_{\text{T1}}| = \tfrac{na}{4}\delta e_{\text{F}} > \tilde{e} \quad \rightarrow \quad a\delta e_{\text{min}} = 511.25\,\text{m} \tag{10}$$

for the servicer at an an orbit altitude of 515 km.
The same error consideration applied in the normal component of the delta-v impacts the truly obtainable magnitude of the relative inclination vector. This is referred as constraint safety #7 in Table 1, and fixes the margin equal to $\tilde{e}/n$ [i.e., 127.81 m at the same orbit height of Eq. (10)], being n the carrier mean motion.
The minimum size of the stable final relative orbit is also limited by passive safety considerations (i.e., constraint safety #5), that ask for a minimum R–N distance of $100 \div 150$ m. By merging all these requirements, the lower bounds reported in Table 2 are obtained.

Finally, the maximum size of the relative orbit is constrained by the Field Of View (FOV) of the camera (i.e., visibility constraints #2 and #3). The worst case scenario occurs at the minimum allowed mean relative longitude value (i.e., $a\delta\lambda_{\text{F}} = 5000$ m). By making use of the Eq. (3) of Reference 16, and by neglecting the correction due to curvature, the following limits are identified:

$$\delta e_{\text{F}} < \tan(6.8^\circ)|\delta\lambda_{\text{F}}| \qquad\qquad \delta i_{\text{F}} < \tan(9.15^\circ)|\delta\lambda_{\text{F}}| \tag{11}$$

and the subsequent values are also collected in Table 2.

It is emphasized that the three final magnitudes $\delta\lambda$, δe, and δi cannot be chosen independently, due to the constraint on the magnitude of the first maneuver. Moreover in Eq. (9) the incorrect value $\Delta\delta\lambda^*$ appears, whereas we are interested in $\Delta\delta\lambda$.
Both these points suggest choosing δe and δi as design parameters, in their domains of feasibility. Consequently, the value of radial component of the first delta-v is given by:

$$\delta v_{\text{R1}} \quad = \quad -\sqrt{\delta v^2 - {\delta v_{\text{T1}}}^2 - {\delta v_{\text{N1}}}^2} \tag{12}$$

and $\Delta\delta\lambda^*$ is then computed using the first line of Eq. (9).
This obtained value influences the choice of κ, so that the final $\delta\lambda_{\text{F}}$ is in its domain of feasibility. The relationship between the obtained relative mean longitude and $\Delta\delta\lambda^*$ of Eq. (6) is provided by:

$$\delta\lambda_{\text{F}} = -1.5(\kappa\pi)\delta a_1 + \Delta\delta\lambda^* \tag{13}$$

where $\delta a_1 = (2/n)\delta v_{\text{T1}}$. Therefore, once fixed δv_{R1} (i.e., fixed δe and δi), κ can be chosen as the odd natural number comprised in:

$$-\frac{5000 - \Delta\delta\lambda^*}{1.5\pi\delta a_1} \leq \kappa \leq -\frac{10000 - \Delta\delta\lambda^*}{1.5\pi\delta a_1} \tag{14}$$

The following remarks can be added when dealing with the final selection of the baseline (i.e., aimed δe and δi):

- Visibility constraints #2 and #3 can be handled as *soft* constraints, since they become less critical when the separation increases. Both differential drag and the choice of a bigger κ contribute to this.

- The magnitude of δi can be small (coherently with its domain) in order to avoid further consumption of delta-v due to a second cross-track burn. Moreover, this allows allocating more delta-v to the tangential and radial components of the first maneuver, which is fruitful for safety constraint #6 and for establishing faster a certain separation.

- Visibility constraints #1 could also be softened since later corrections can be accomplished before switching to visual-based relative navigation (at the cost of further delta-v consumption).

An example of feasible baseline can be obtained by choosing the following values:

$$\begin{array}{rcl} a\delta e_{\mathrm{F}} & = & 590\,\mathrm{m} \\ a\delta i_{\mathrm{F}} & = & 400\,\mathrm{m} \end{array} \tag{15}$$

leading to these nominal delta-v magnitudes:

$$\begin{array}{l} \delta\mathbf{v}_1 = (\delta v_{\mathrm{R1}}, \delta v_{\mathrm{T1}}, \delta v_{\mathrm{N1}})^{\mathrm{T}} = (-1.329250, -0.162718, 0.441269)^{\mathrm{T}}\,\mathrm{m/s} \\ \delta\mathbf{v}_2 = (\delta v_{\mathrm{R2}}, \delta v_{\mathrm{T2}}, \delta v_{\mathrm{N2}})^{\mathrm{T}} = (-1.329250, +0.162718, 0.0)^{\mathrm{T}}\,\mathrm{m/s} \end{array} \tag{16}$$

The admissible values of κ to satisfy Eq. (14) are $[1, 3]$. It is emphasized that, since the delta-vs do not depend on this choice [see Eq. (9)], the same delta-v plan remains valid in the case that any anomaly prevented executing the second maneuver. Besides, a delay in the execution of such maneuver causes the aimed $\delta\lambda_{\mathrm{F}}$ to increase according to Eq. (13).
Figure 2 shows the nominal relative trajectory obtained with $\kappa = 3$ in the RTN frame. At this level of the analysis no disturbances are included in the ROE propagation. The solid lines in the R–N, R–T, and N–T views define the area of the FOV of the camera mounted on the BIROS spacecraft.

Before dealing with the verification of the chosen baseline with respect to system's uncertainties, a final design problem needs to be addressed. It concerns the sign of the final relative drift when the executed delta-vs differ from the nominal commanded ones. This topic is relevant since we cannot estimate the truly executed first impulse before accomplishing the second maneuver.
Being the drift linked to the tangential components of the delta-vs, at a design level we can assume that no error is accomplished on the radial and normal components of Eq. (16). When the truly executed first tangential maneuver is given by:

$$\delta v^*_{\mathrm{T1}} = \delta v_{\mathrm{T1}} + e_1 \tag{17}$$

a possible critical situation can arise if e_1 reduces the magnitude of δv^*_{T1} (i.e., $e_1 > 0$). In this case, the second tangential maneuver would produce a drift reversal resulting in a drift of the picosatellite towards the servicer. Since the delta-v values are computed according to Eq. (9), increasing the baseline value of $\Delta\delta e$ does not remove this problem.
A mitigation of this issue can be achieved by commanding the following nominal tangential delta-v for the second maneuver instead:

$$\delta v^*_{\mathrm{T2}} = \delta v_{\mathrm{T2}} + e_2 - |p| \tag{18}$$

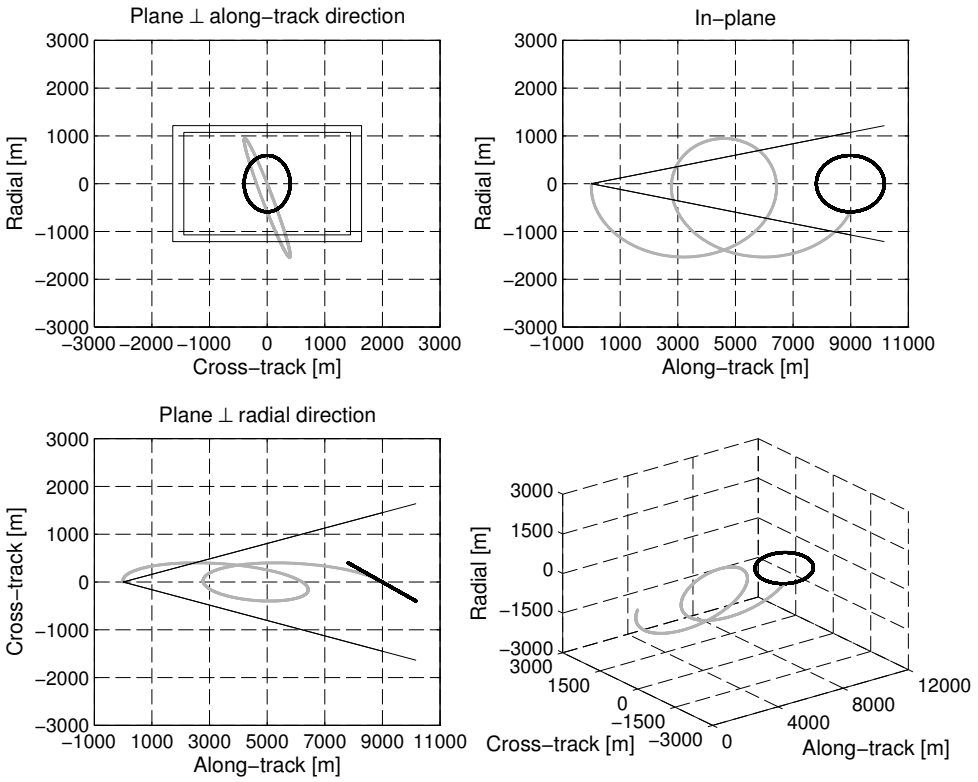

Figure 2. Example of the feasible baseline of Eq. (15) **with delta-vs of Eq.** (16)

where the parameter p has to be sized in order to properly determine the strength of the drift reduction. The error in the tangential component of the second maneuver e_2 increases the magnitude of the drift reduction whenever $e_2 > 0$.

This approach exploits the particular structure of our separation design formulation. It can be shown, in fact, that given the two maneuvers spaced by $\kappa\pi$ and having $|\delta v_{\mathrm{R1}}| = |\delta v_{\mathrm{R2}}|$ [see Eq. (9)], the final phase of the relative eccentricity vector ξ remains the same whatever value of δv^*_{T1} and δv^*_{T2} are performed. Moreover, the final magnitude of the relative eccentricity vector is given by:

$$a\delta e^*_{\mathrm{F}} = \frac{1}{n}\sqrt{4({\delta v^*_{\mathrm{T1}}}^2 + {\delta v^*_{\mathrm{T2}}}^2 - 2\delta v^*_{\mathrm{T1}}\delta v^*_{\mathrm{T2}})} \tag{19}$$

Hence, the parameter p can be chosen such that the sign of the final relative semi-major axis δa^*_{F} is negative even with the greatest under performance of the POD device. At the same time, p is limited by the need to perform at least some drift reduction. These two statements can be formalized as:

$$\begin{cases} \delta v_{\mathrm{T2}} - e_2 - |p| > 0 & \rightarrow \quad \delta v^*_{\mathrm{T2}} > 0 \\ \delta v_{\mathrm{T2}} + e_2 - |p| \leq |\delta v_{\mathrm{T1}}| - e_1 & \rightarrow \quad \delta a^*_{\mathrm{F}} < 0 \end{cases} \tag{20}$$

which lead to the following design range for p:

$$e_1 + e_2 \leq |p| < \frac{na}{4}\delta e_{\mathrm{F}} - e_2 \tag{21}$$

having used that $\delta v_{\mathrm{T2}} = |\delta v_{\mathrm{T1}}| = na\delta e_{\mathrm{F}}/4$.

To conclude this section, the choice of the aimed final relative orbit shall be accomplished by selecting the values $(a\delta e_{\mathrm{F}}, a\delta i_{\mathrm{F}}, p)$ that allows satisfying all the constraints considered so far. Moreover

one should verify that the final $a\delta e_{\mathrm{F}}^{*}$ from Eq. (19) meets the passive safety requirement (i.e., safety constraint #5 in Table 1), despite the presence of p. Finally, the case of over performance of the POD device shall be taken into account. The maximum drift imparted by the first maneuver shall not bring to evaporation, having weakened the drift reduction through p.

MONTE CARLO SIMULATION

In order to validate the risk of the planned maneuver strategy, some Monte Carlo (MC) simulations have been performed. It should be noted, that all simulation runs were executed generating 100000 samples but only 1000 are plotted for readability. The simulation uses the following dispersion parameters:

- The dispersion of the POD mechanism is unknown, hence a pessimistic dispersion with a standard deviation of 10% of the overall delta-v is assumed. This is expressed by multiplying the first maneuver by a factor f_1, which has a mean value of 1 and a σ of 0.1.

- The execution accuracy of the BIROS propulsion system is unknown at this stage. Similarly to the POD mechanism a dispersion of 5% is assumed. This is expressed by multiplying the second maneuver by a factor f_2, which has a mean value of 1 and a σ of 0.05. It is noted, that it will be possible to accurately calibrate the BIROS thrusters during the commissioning phase, hence this value might change at a later stage.

- The BIROS satellite is known to have an attitude control accuracy of 30 arcsec. This is expressed by multiplying both maneuvers by a rotation matrix for small angles, where the quantities ϵ_x, ϵ_y and ϵ_z have a mean value of 0 and a σ of 30". The simulated delta-vs $\delta v_{\mathrm{R}i}^{\mathrm{s}}$ for maneuvers $i = 1, 2$ are obtained by:

$$\begin{pmatrix} \delta v_{\mathrm{R}i}^{\mathrm{s}} \\ \delta v_{\mathrm{T}i}^{\mathrm{s}} \\ \delta v_{\mathrm{N}i}^{\mathrm{s}} \end{pmatrix} = f_i \begin{pmatrix} 1 & \epsilon_{zi} & -\epsilon_{yi} \\ -\epsilon_{zi} & 1 & \epsilon_{xi} \\ \epsilon_{yi} & -\epsilon_{xi} & 1 \end{pmatrix} \begin{pmatrix} \delta v_{\mathrm{R}i} \\ \delta v_{\mathrm{T}i} \\ \delta v_{\mathrm{N}i} \end{pmatrix} \tag{22}$$

- The effect of the differential drag on the relative mean longitude and relative smi-major axis can be computed as[9] :

$$a\delta\lambda(t) = \frac{3}{4n^2}\Delta B\rho v^2 \left(u(t) - u_0\right)^2 \tag{23}$$

$$a\delta a(t) = -\frac{1}{n^2}\Delta B\rho v^2 \left(u(t) - u_0\right) \tag{24}$$

  Considering the physical properties of BIROS (cross-section of 0.8 m $\times$ 0.6 m at nominal attitude, weight of 140 kg) and the picosatellite (cross-section of 0.1 m $\times$ 0.1 m, weight of 1 kg) with an assumed atmospheric density of $\rho = 1\mathrm{g/km}^3$ and a drag-coefficient of $c_d = 2.3$, the relative ballistic coefficient can be determined as $\Delta B = 0.0151\ \mathrm{m}^2/\mathrm{kg}$. Nevertheless the atmospheric density, the true effective cross-section (due to attitude maneuvers) and the true weight of the satellites (e.g. due to fuel consumption) are difficult to predict. Hence an uncertainty of the differential drag with $\sigma = 20\%$ is applied in the Monte Carlo simulations.

Using the baseline maneuvers determined above [see Eq. (16)] and assuming a maximum under performance of 3σ for both maneuvers, a reduction value of $p = 0.0732231$ m/s is determined. A first Monte Carlo simulation was executed without including the effect of differential drag in order to verify if the final relative semi-major axis $a\delta a$ can assume a positive value, which would result in the satellites drifting towards each other. As can be seen in Figure 3, in none of the cases $a\delta a$ is positive. In the following figures each dot represents one sample of the simulation. In Figures 3, 4 and 5, the remaining relative semi-major axis after the second maneuver is plotted against the mean separation in tangential direction. The left plots show the situation directly after the second maneuver, while the right ones show the development 24 hours later, when the final maneuver is about to be performed. The bold lines at $a\delta\lambda = 5000$ m and $a\delta\lambda = 10000$ m show the thresholds of separability by radar tracking and of visibility by the BIROS onboard camera.

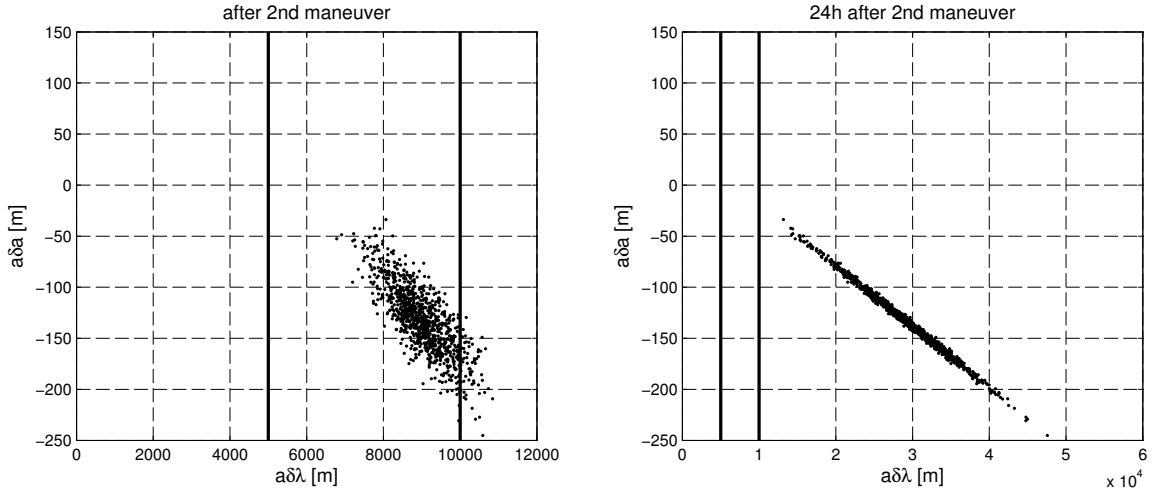

Figure 3. Residual $a\delta a$ in dependence of mean tangential separation ($p = 0.0732231$ m/s, no differential drag).

A second simulation run was executed with the differential drag effect taken into account and the reduction value p set to 0 in order to demonstrate the effect of the differential ballistic coefficient on the remaining drift. As can be see in Figure 4, in more than 40% of the cases $a\delta a$ is positive. In about 3.6 % of the cases the drift induced by the relative semi-major axis has led to a reduction of the mean tangential separation to less than 5000 m and in 0.3 % of the cases the BIROS satellite even passed the picosatellite in tangential direction. This undesired approach means, that the two spacecraft could not be distinguished by radar tracking and a relative orbit determination becomes impossible.

This demonstrates, that the differential drag effect alone is not enough to prevent an approach of the satellites and a reduction of the tangential component of the second maneuver is necessary. The parameter p has to be tuned such, that the likelihood of an approach of the satellites (i.e. $a\delta a > 0$), as well as that of an evaporation of the formation is minimized. A threshold of 50 km is defined as formation evaporation, since below that distance the formation can be recovered without too much effort from ground. Table 3 shows the probabilities of an approaching drift and formation evaporation for a selected range of p. The probability is computed by the number of events ($a\delta a > 0$ or $a\delta\lambda > 50$ km) divided by the total number of simulation runs. It is not possible to eliminate both the risks, but with a value of $p = 0.55$ m/s a minimum of the combined risk is found.

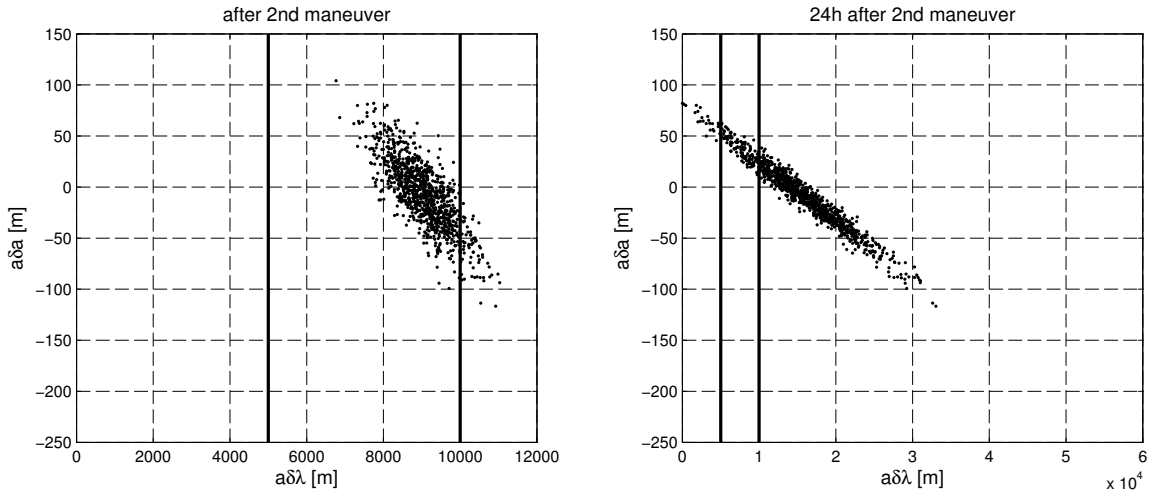

Figure 4. Residual $a\delta a$ in dependence of mean tangential separation ($p = 0$ m/s, drag included).

Table 3. Selection of the reduction value p for the nominal guidance plan of Eq. (16).

p [m/s]	$a\delta a > 0$ m	$a\delta\lambda > 50$ km
0.00	41.72 %	0.00 %
0.01	22.74 %	0.00 %
0.02	9.96 %	0.00 %
0.03	3.07 %	0.00 %
0.04	0.78 %	0.00 %
0.05	0.12 %	0.02 %
0.055	0.06 %	0.03 %
0.06	0.00 %	0.11 %
0.07	0.00 %	1.23 %
0.08	0.00 %	1.30 %

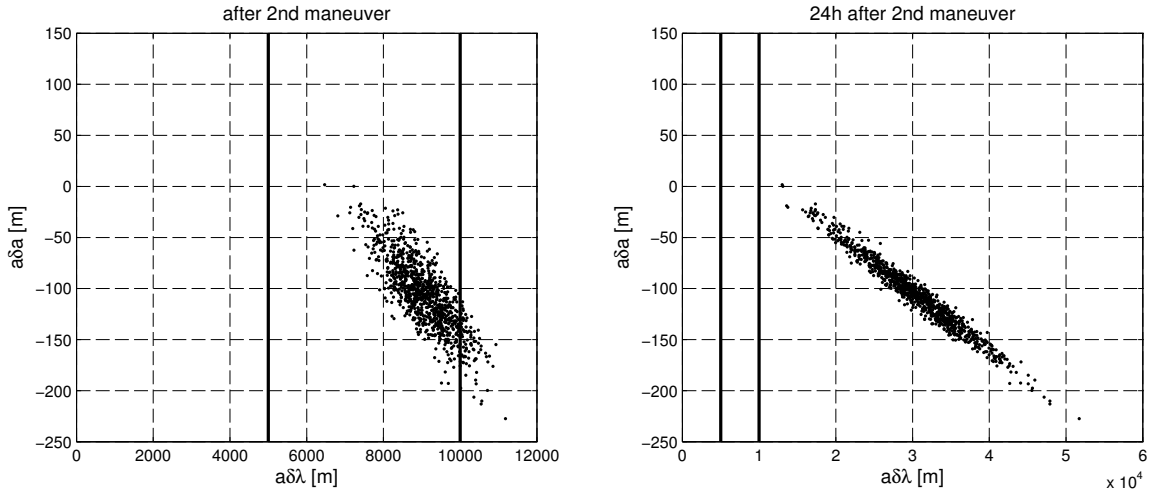

Figure 5. Residual $a\delta a$ in dependence of tangential separation ($p = 0.55$ m/s, drag included).

As stated above, with the selected $p = 0.55$ m/s an approach of the satellites cannot be excluded. This is confirmed by Figure 5, which shows, that a very small number of cases with $a\delta a > 0$ remains. Hence it has to be checked, if the passive safety is sufficient in order to avoid a collision in case of an approach of the two spacecraft in tangential direction. Therefore the magnitudes of the relative eccentricity $a\delta e$ and relative inclination $a\delta i$ are shown in Figure 6. The limits for safety (150 m in both R and N) and visibility (596 m R, 805 m N) are indicated in the plot. It can be seen, that in rare (0.02 %) cases the limits for visibility are violated, but the safety margin for passive stability is always fulfilled.

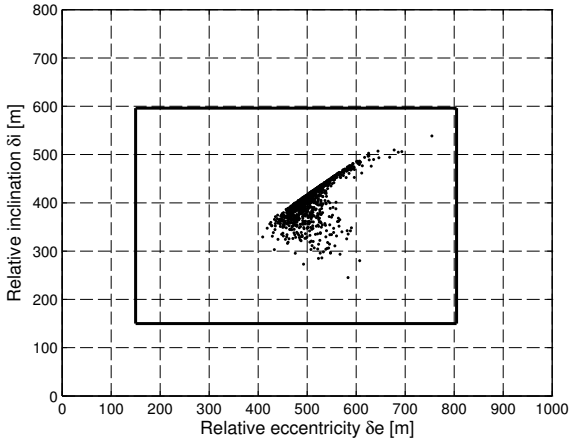

Figure 6. Relative eccentricity $a\delta e$ and inclination $a\delta i$ after 2nd maneuver.

The passive safety can be verified as well by regarding the minimum distance of the two spacecraft in the T = 0 plane. Under the assumption that $a\delta a = 0$ it is defined as:[9]

$$\delta r_{nr}^{\min} = \frac{\sqrt{2}a\,|\delta \boldsymbol{e} \cdot \delta \boldsymbol{i}|}{\left(\delta e^2 + \delta i^2 + |\delta \boldsymbol{e} + \delta \boldsymbol{i}| \cdot |\delta \boldsymbol{e} - \delta \boldsymbol{i}|\right)^{1/2}} \tag{25}$$

This equation shows the importance of parallel or anti-parallel relative eccentricity and inclination vectors due to the scalar product of those vectors. In Figure 7 the minimum cross-track distance is plotted in dependence of the residual $a\delta a$. As stated above Eq. 25 is valid for $a\delta a = 0$, but in most cases $a\delta a$ is negative, thus the picosatellite is drifting towards greater separations. Only in the rare event of severe under-performance of the release mechanism, $a\delta a$ is close to 0. In these cases $\delta r_{nr}^{\min}$ is at around 150 m (see Figure 7), which means, that the passive safety of the formation is still guaranteed.

Finally it has to be verified, that a collision risk before the execution of the second maneuver can be ruled out. In case of a severe under-performance of the spring mechanism, the two spacecraft could approach after one revolution in case not enough tangential separation is built up. Therefore the tangential separation at the nearest crossing of the R $= 0$ plane is examined. Figure 8 shows that distance in dependence of the performance factor f_1 of the separation mechanism. It can be seen, that the behavior is almost linear, but even in the case of a 3σ under-performance ($f_1 < 0.7$), the tangential separation is still larger than 1600 m and no collision risk exists.

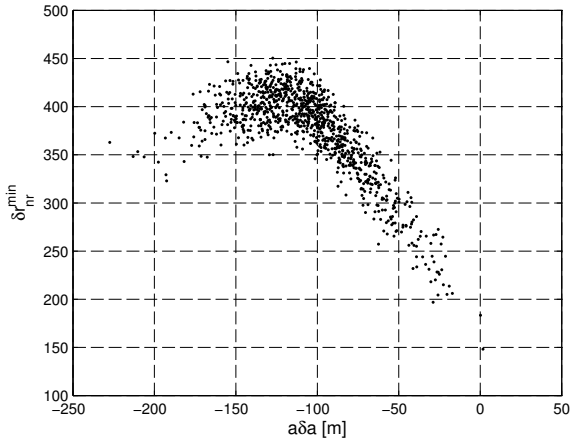

Figure 7. Minimum cross-track distance in dependence of the final $a\delta a$.

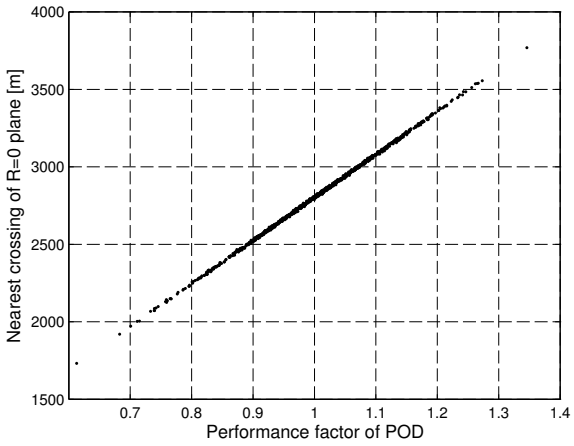

Figure 8. Nearest crossing of the R $= 0$ plane.

CONCLUSION

This paper addressed the design and the consequent feasibility analysis of the in-orbit release of a picosatellite from a small satellite carrier in low Earth orbit. This research embodies the prerequisite to the execution of the Autonomous Vision Approach Navigation and Target Identification (AVANTI), scheduled for 2015. To this aim, a comprehensive overview of the mission requirements and of the operational aspects relevant to the mission safety has been provided.

The peculiar scenario of aiming at a mid-range stable formation while employing a release mechanism that provides a large and strongly uncertain separation delta-v, demanded the complement of the well-known passive safety concept, based on the relative eccentricity/inclination vector separation, with some further feasibility criteria. Specifically, the first one concerns the achievement of the minimum along-track separation to exploit a radar tracking campaign to perform some relative orbit determination. Within our scenario, in fact, this represents the only available source of navigation information. The second criterion, closely related to the first one, asks the unavoidable residual drift to increase the relative separation, regardless of the magnitude and of the nature of the

system's uncertainties. Finally, the last feasibility criterion is to reduce at minimum the probability of a formation evaporation, thus posing a condition in contrast with the first two.

This paper proposed a formalization of all these aforementioned safety requirements that allowed addressing them already at the design level. This was accomplished by exploiting the powerful framework of the relative orbital elements. Moreover, our study supported such an investigation with a numerical analysis which included several sources of uncertainty, representative of the behavior of the space segment. As a result, a realistic assessment of the feasibility of a double-impulse guidance plan in contrast to the risk of formation evaporation has been obtained.

This research focused on a double-impulse guidance strategy, where the first maneuver is provided by the deployment mechanism, whereas the second one is accomplished by the thrusters' system of the carrier satellite. Nevertheless, prior to the ultimate selection of the final mission plan, an analysis of the realistic performance of a multi-impulse separation scheme as to be accomplished as well. According to the carrier thrusters' system, the involvement of a larger number of maneuvers allows distributing the needed delta-v over more but smaller burns. At a planning level, a larger range of relative configurations can be exploited in the intermediate phases, since only the final relative orbit is subjected to the complete set of constraints. The introduction of additional maneuvers can lead to a larger delta-v consumption.

NOTATION

a	semimajor axis of the servicer satellite
$\Delta\bullet$	finite variation of a quantity
$\delta\bullet$	relative quantity
$\delta\boldsymbol{\alpha}$	nondimensional relative orbital elements ROE set
$\delta\mathbf{e}$	nondimensional relative eccentricity vector
$\delta\mathbf{i}$	nondimensional relative inclination vector
$\delta\lambda$	nondimensional relative longitude
δv_{R},δv_{T},δv_{N}	instantaneous velocity changes in local RTN frame
e	eccentricity of the servicer satellite
e_i	delta-v error on the i-th tangential component
ϵ_{xi}, ϵ_{yi}, ϵ_{zi}	Simulated errors of the BIROS attitude control during maneuver i
f_i	Simulated performance factor of maneuver i
i	inclination of the servicer satellite
φ	argument of latitude of the relative perigee
n	mean angular motion of the servicer satellite
p	real number
θ	argument of latitude of the relative ascending node
κ	odd natural number
u	mean argument of latitude of the servicer satellite
ω	argument of perigee of the servicer satellite
Ω	longitude of ascending node of the servicer satellite
ξ	phase of the relative eccentricity vector

REFERENCES

[1] H. Reile, E. Lorenz, and T. Terzibaschian, "The FireBird Mission - A Scientific Mission for Earth Observation and Hot Spot Detection," *Small Satellites for Earth Observation, Digest of the 9th Inter-*

national Symposium of the International Academy of Astronautics, Berlin, Germany, Wissenschaft und Technik Verlag, 2013. ISBN 978-3-89685-574-9.

[2] B. Engberg, J. Ota, and J. Suchman, "The OPAL Satellite Project: Continuing the Next Generation Small Satellite Development," *Proceedings of the 9th Annual AIAA/US Conference on Small Satellites*, Logan, Utah, USA, 1995.

[3] J. Puig-Suari, C. Turner, and W. Ahlgren, "Development of the standard CubeSat deployer and a CubeSat class PicoSatellite," *Aerospace Conference, 2001, IEEE Proceedings*, Vol. 1, 2001, pp. 347–353, 10.1109/AERO.2001.931726.

[4] P. G. Ballard, A. Meza, S. Ritterhouse, T. Schaffer, C. Conley, C. Taylor, D. D. D. Atkine, and J. C. McLeroy, "Small Satellite Deployments From STS116 - Development Of New Manned Spaceflight Deployment Systems," *Proceedings of the AIAA/USU Conference on Small Satellites, Technical Session III: Launch & Propulsion Systems*, 2007, http://digitalcommons.usu.edu/smallsat/2007/all2007/19/.

[5] J. C. Springmann, A. Bertino-Reibstein, and J. W. Cutler, "Investigation of the on-orbit conjunction between the MCubed and HRBE CubeSats," *Aerospace Conference, 2013 IEEE*, 2013, pp. 1–8, 10.1109/AERO.2013.6497127.

[6] "Poly Picosatellite Orbital Deployer Mk III ICD," tech. rep., The CubeSat Program Std., 2007, http://cubesat.org/images/LaunchProviders/.

[7] P. Bodin, R. Noteborn, R. Larsson, T. Karlsson, S. D'Amico, J. S. Ardaens, M. Delpech, and J. C. Berges, "Prisma Formation Flying Demonstrator: Overview and Conclusions from the Nominal Mission," No. 12-072, Breckenridge, Colorado, USA, 35th Annual AAS Guidance and Control Conference, 2012.

[8] S. Persson, S. D'Amico, and J. Harr, "Flight Results from PRISMA Formation Flying and Rendezvous Demonstration Mission," Prague, Czech Republic, 61st International Astronautical Congress, 2010.

[9] S. D'Amico, *Autonomous Formation Flying in Low Earth Orbit*. PhD thesis, Technical University of Delft, The Netherlands, Mar. 2010.

[10] A. Harting, C. K. Rajasingh, M. C. Eckstein, A. F. Leibold, and K. N. Srinivasamurthy, "On the collision hazard of colocated geostationary satellites," No. 88-4239, Minneapolis, USA, AIAA/AAS Astrodynamics conference, 1988.

[11] O. Montenbruck, M. Kirschner, S. D'Amico, and S. Bettadpur, "E/I-Vector Separation for Safe Switching of the GRACE Formation," *Aerospace Science and Technology*, Vol. 10, No. 7, 2006, pp. 628–635. doi: 10.1016/j.ast.2006.04.001.

[12] S. D'Amico and O. Montenbruck, "Proximity Operations of Formation Flying Spacecraft using an Eccentricity/Inclination Vector Separation," *Journal of Guidance, Control and Dynamics*, Vol. 29, No. 3, 2006, pp. 554–563.

[13] J. Spurmann and S. D'Amico, "Proximity Operations of On-Orbit Servicing Spacecraft using an Eccentricity/Inclination Vector Separation," Sao Jose dos Campos, Brazil, 22nd International Symposium on Spaceflight Dynamics, 2011.

[14] G. Gaias and S. D'Amico, "Impulsive Maneuvers for Formation Reconfiguration using Relative Orbital Elements," *Journal of Guidance, Control, and Dynamics*, 2013. accepted for publication.

[15] R. Kahle, M. Weigel, M. Kirschner, S. Spiridonova, E. K. E, and K. Letsch, "Relative Navigation to Non-cooperative Targets in LEO: Achievable Accuracy from Radar Tracking Measurements," Munich, Germany, 5th International Conference on Spacecraft Formation Flying Missions and Technologies, 2013.

[16] S. D'Amico, J. S. Ardaens, G. Gaias, H. Benninghoff, B. Schlepp, and J. L. Jørgensen, "Noncooperative Rendezvous Using Angles-Only Optical Navigation: System Design and Flight Results," *Journal of Guidance, Control, and Dynamics*, Vol. 36, No. 6, 2013, pp. 1576–1595. doi: 10.2514/1.59236.

[17] W. H. Clohessy and R. S. Wiltshire, "Terminal Guidance System for Satellite Rendezvous," *Journal of the Aerospace Sciences*, Vol. 27, No. 9, 1960, pp. 653–658.

[18] S. D'Amico, "Relative Orbital Elements as Integration Constants of Hill's Equations," DLR-GSOC TN 05-08, Deutsches Zentrum für Luft- und Raumfahrt, Oberpfaffenhofen, Germany, Dec. 2005.